Published by CERN in the Proceedings of the CAS-CERN Accelerator School: Power Converters, Baden, Switzerland, 7–14 May 2014, edited by R. Bailey, CERN-2015-003 (CERN, Geneva, 2015)

Power Converters for Cycling Machines

J-F. Bouteille
ESRF, Grenoble, France

Abstract
Cycling accelerators require power converters that are capable of storing the energy that oscillates between lattice magnets and the converter during the acceleration process. This paper presents the basic requirements for such systems and reviews the various electrical circuits that have been used for a variety of differing applications. The designs currently used for fast-, medium- and slow-cycling accelerators are presented.

Keywords
Energy; power; acceleration; flicker; energy exchange; waveform.

1 Introduction

Some of the material presented in these proceedings is concerned with converters which supply direct current to the magnet loads. This is relevant to the storage ring, in which the particle momentum is fixed or where its variation with time is so slow that the energy increase in the magnets is smaller or of the same order as the resistive energy loss; in such circumstances, the converters can be regarded as variable-amplitude d.c. systems. However, in most true synchrotrons, which accelerate the charged particle beam, the magnetic fields in the bending and focusing elements (if these are part of a separated function lattice) are required to be raised in a relatively short time, from the low amplitude required at beam injection to a maximum value corresponding to peak beam energy; the fields then need to be reduced in as short a time as possible, so as to be ready to accept the next pulse of injected beam. Thus, these cycling accelerators require power converters that are capable of delivering the appropriate cycling waveform.

As the accelerator magnets cycle from the injection to peak field, energy is transferred from the power converter to the magnet gap; during the deceleration phase, this magnetic energy has to be removed from the magnet. In the case of a d.c. accelerator, this process occurs during switch-on and, far later, during the power-down of the converters. The stored energy is small compared to the resistive loss in the magnet during any extended period of d.c. operation, and hence this 'reactive power' is not considered in the power supply specification. However, in a cycling accelerator, the largest component of energy supplied from the converter to the magnets is usually the magnetic energy associated with the field amplitude. It is therefore significantly more efficient to recover that energy during the deceleration phase and store it for the next acceleration cycle. Hence, a suitable energy storage system is an essential part of a converter for a cycling accelerator, and this requirement is central to the design and specification of such equipment. The nature of suitable engineering schemes depends on the cycling frequency specified for the accelerator; these can vary from less than 1 Hz for the large synchrotrons associated with particle physics, to 50 Hz for small- to medium-sized accelerators. The details of the most suitable circuits are discussed in the following.

2 The choice of waveform

2.1 Accelerator requirements

The simplest waveform that could be envisaged for a cycling system is 'conventional' alternating current. However, consideration of the requirements for particle acceleration indicates that this is highly inappropriate. This is explained in Fig. 1. Injection occurs at low field and the particles are then

http://dx.doi.org/10.5170/CERN-2015-003.171

accelerated to peak energy, at the maximum of the sine wave; the acceleration occurs only during the positive part of the cycle. The simple a.c. waveform shown in the figure produces major disadvantages:

- less than one-quarter of the cycle is used for acceleration,
- there is an unnecessarily large r.m.s. current, as the negative part of the wave is superfluous,
- therefore there are high resistive and a.c. losses,
- there is a high magnetic field variation with time at injection (see the following),
- The energy is exchanged 4 times per cycle as only two are required.

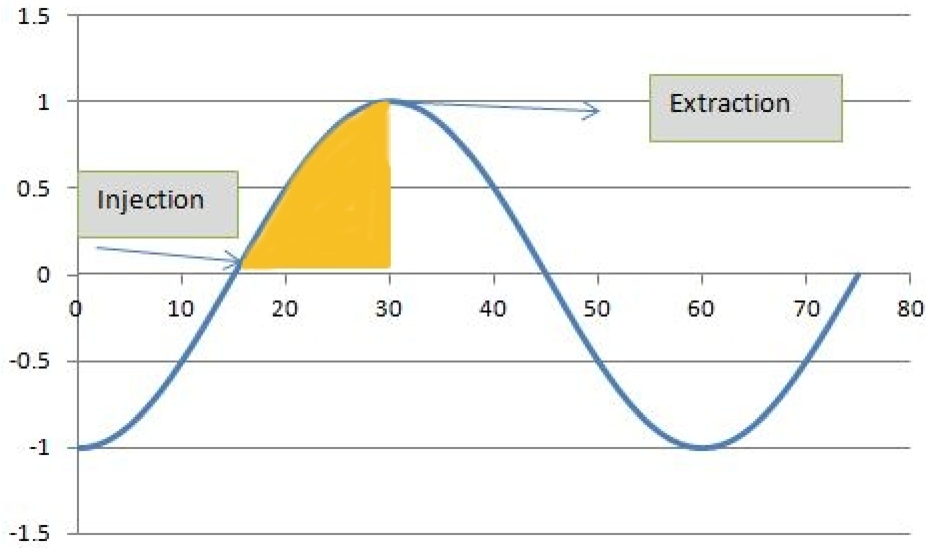

Fig. 1: Simple a.c. is an inappropriate waveform for a cycling accelerator. The simple alternating current wave is not used without biased current.

Before examining other possible waveforms in detail, it is worthwhile examining the detailed waveform requirements of the cyclic particle accelerator.

2.1.1 RF system

The radio frequency system provides the voltage necessary to accelerate the particles, or, where the particles are losing energy due to synchrotron radiation, to replace that loss and maintain the beam at the required momentum.

2.1.1.1 Acceleration

- Particle momentum (rigidity)

$$mv \propto B; \tag{1}$$

- RF accelerating voltage

$$V_{\rm rf} \propto \mathrm{d}B/\mathrm{d}t; \tag{2}$$

- RF power

$$P = k_1 V_{\rm rf} I_{\rm beam} + k_2 (V_{\rm rf})^2 \tag{3}$$

= (power transferred to beam) + (loss into cavities);

where

- mv is the momentum of a particle mass m;
- B is the magnetic flux density in the bending magnets;

– I_{beam} is the beam current;

– k_1 and k_2 are constants fixed by the RF system and accelerator design.

Any discontinuity in dB/dt would call for a step change in RF voltage and power and could generate beam instabilities, leading to possible beam loss.

Additionally, the particle beam is held in a potential well, created by the RF voltage, in a mechanism known as 'phase stability'. The trapped particles move within that potential well, executing 'synchrotron oscillations'. The frequency of these oscillations (the 'synchrotron frequency') is one of the fundamental parameters of the accelerator and is proportional to dB/dt. Large values of this frequency can also cause resonant beam loss, and this places a further constraint on the field gradient, particularly at injection (see the following).

2.1.1.2 Synchrotron radiation

This radiation is emitted by ultrarelativistic particle beams (electrons at E ~ 1 GeV; protons at E ~ 1 TeV) when bent in a magnetic field:

– synchrotron radiation loss $\propto B^2E^2$, (4)

– for a constant radius accelerator $\propto B^4$, (5)

– V_{rf} to maintain energy $\propto B^4$, (6)

where E is the energy of the circulating beam.

The magnet waveform therefore needs to have no discontinuities in amplitude (effectively impossible with an inductive load) or gradient. To limit the maximum RF voltage that needs to be generated by the RF amplifier (and therefore to limit its power ratings), the maximum value of dB/dt should not greatly exceed the average required over the acceleration cycle.

2.1.2 Field gradient at injection

The variation of magnetic flux density with time generates eddy currents in any conducting material located within the field. In a cycling accelerator, eddy currents will occur predominantly in the walls of a metallic vacuum vessel, with smaller eddy currents present in the magnet poles themselves. These currents generate magnetic field disturbances:

– negative dipole field—reduces main field magnitude;

– negative sextupole field—generates negative chromaticity and could drive resonances.

The magnitude of these unwanted disturbances is inversely proportional to the beam momentum, which is, of course, determined by the dipole magnetic field, B. Hence the effect of eddy currents is proportional to

$$(1/B)(dB/dt), \text{ expressed as } \dot{B}/B \tag{7}$$

It should be noted that the synchrotron frequency is determined by the same ratio.

This parameter, the ratio of the field gradient to the field magnitude, is most critical at injection, when field and beam momentum are low and when the beam is being 'captured' into its correct synchronous phase. This situation is illustrated in Fig. 2.

It will be seen that the value of (1/B)(dB/dt) will be one of the determining factors on which the waveform suitability is judged.

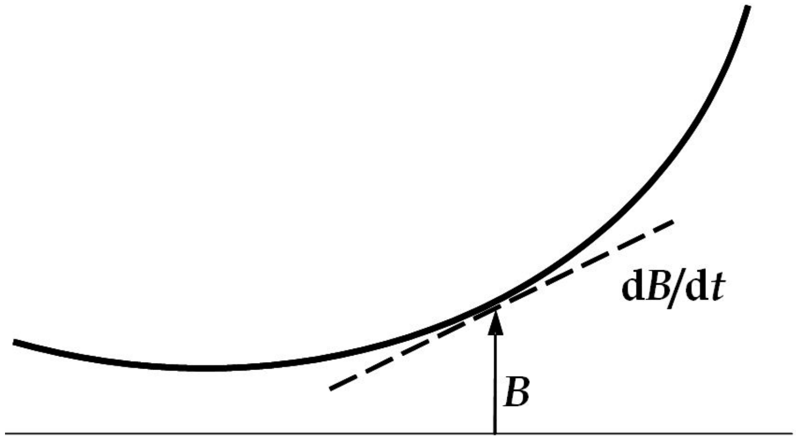

Fig. 2: Field gradient and magnitude at injection

2.1.3 Discontinuous operation

In some situations, the accelerator may only be required to undertake an acceleration cycle at time intervals that are much longer than the normal cycle time. For example, the circulating beam in a storage ring may decay very slowly with time. To maintain constant beam current, which is very valuable to experimenters, the booster synchrotron which feeds the main ring is needed to operate in 'top-up mode', in which the beam is only accelerated and injected once every '*n*' booster cycles, with the value of *n* varying according to the operational details of the storage ring. The booster could be operated continuously whatever time delay is required between injection pulses, but this results in unnecessary power consumption. Hence it is most efficient if the power converter can deliver an excitation waveform that allows discontinuous operation at intervals determined by the rate of loss of the stored beam, as illustrated in Fig. 3.

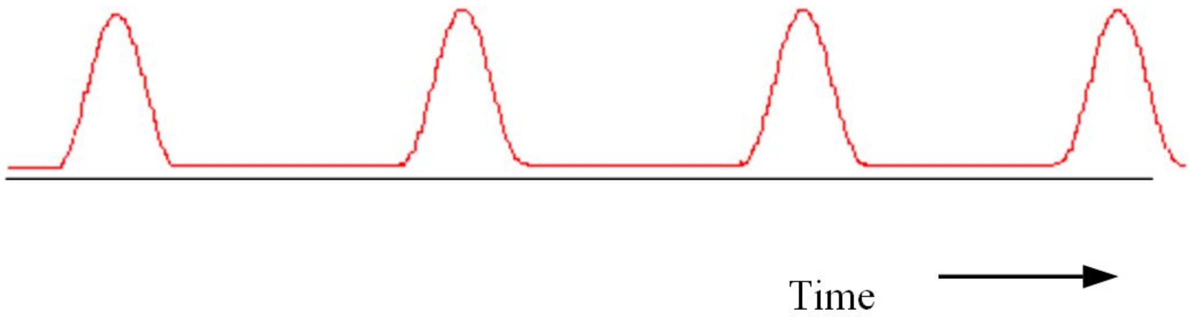

Fig. 3: Discontinuous acceleration cycles as used for 'top-up' injection; note that the delay between cycles is much in excess of the actual cycle time. Several strategies have been observed among top-up machines: at fixed interval (every x minutes or seconds) it is called dt (Diamond, APS); at fixed beam current decay (as soon as the I beam has decreased by x%) it is called dI (SLS, Elettra, Soleil, Bessy, Spring8, Petra).

2.2 Possible waveforms

Having established that a normal alternating current is not suitable for powering a cyclic accelerator and having examined the criteria against which waveforms should be judged, a number of more suitable waveforms can be considered.

2.2.1 Linear ramp

A linear field ramp and associated waveforms are shown in Fig. 4. It can be seen that the uniform gradient throughout the cycle results in a very high value of $(1/B)(\mathrm{d}B/\mathrm{d}t)$ at injection when the field magnitude is low, and some form of smooth transition into the ramp (the 'front porch') would be necessary.

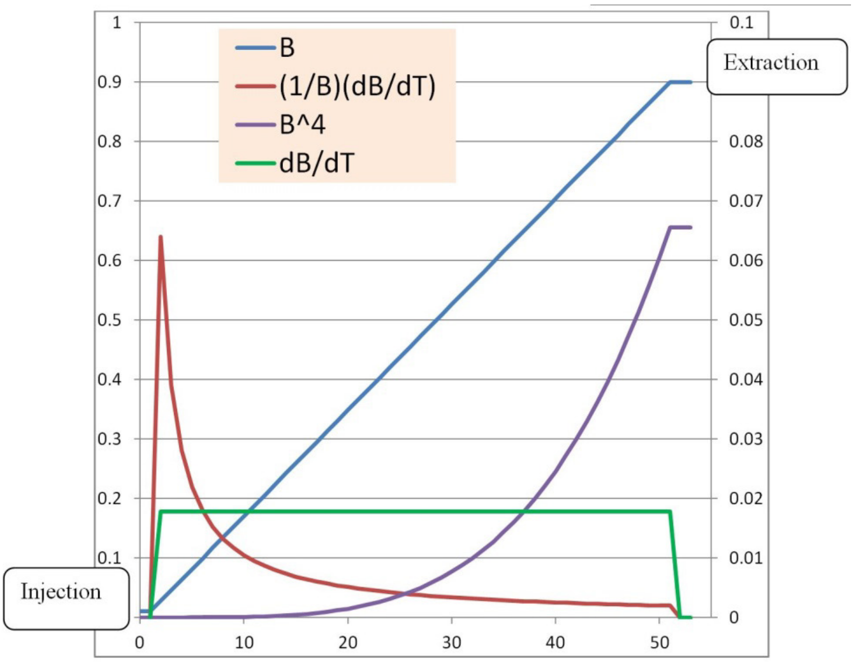

Fig. 4: A linear field ramp between injection and high energy (extraction) (B). Also shown is the gradient ($\mathrm{d}B/\mathrm{d}t$), B dot over B [$(1/B)(\mathrm{d}B/\mathrm{d}t)$], and the function determining synchrotron radiation loss (B^4).

2.2.2 *Biased sine wave*

This waveform, shown in Fig. 5, is based on the use of a half sine wave with a direct current bias of equal magnitude to the sine wave's peak value.

It can be seen that the biased sine wave provides a lower maximum value of $(1/B)(\mathrm{d}B/\mathrm{d}t)$ at injection compared to the linear ramp. However, the variation of gradient during the cycle has a higher maximum value than that produced by the linear variation and, hence, higher RF voltage would be required. Additionally, higher RF power would be needed if the beam was emitting synchrotron radiation, as the integrated value of the B^4 curve is higher.

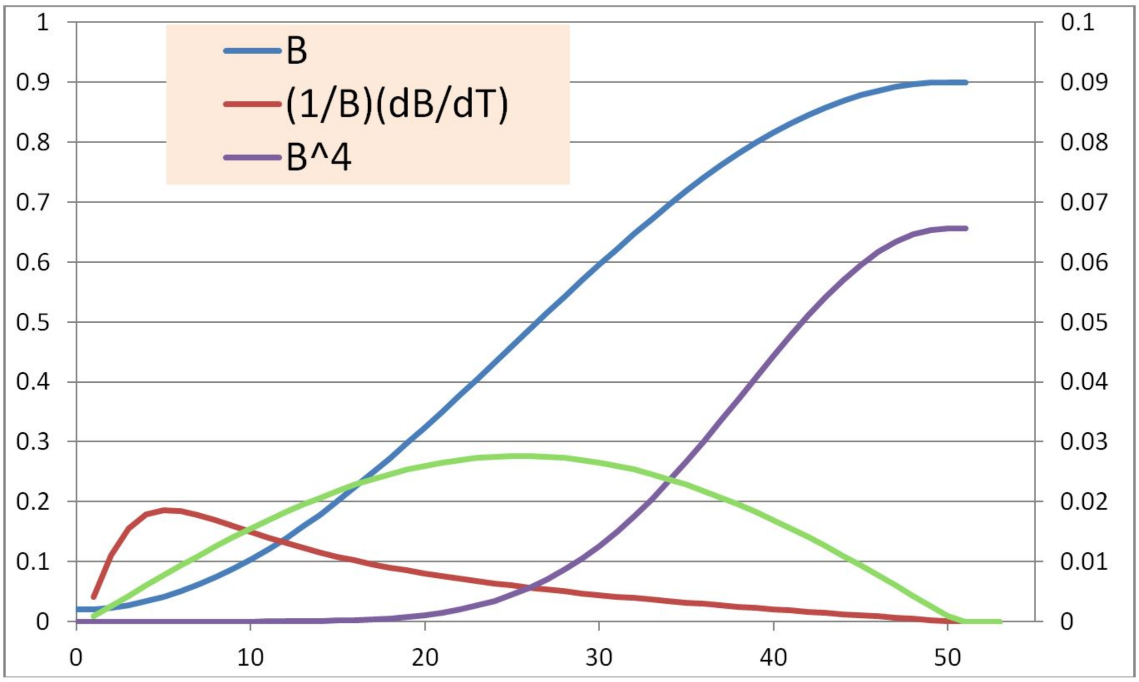

Fig. 5: A biased sine-wave field variation between injection and high energy (extraction) (B). Also shown is the gradient ($\mathrm{d}B/\mathrm{d}t$), B dot over B [$(1/B)(\mathrm{d}B/\mathrm{d}t)$] and the function determining synchrotron radiation loss (B^4).

2.2.3 'Custom specified' waveform

A better alternative to either of the two waveforms presented in Figs. 4 and 5 would be to have a variation with time that could be specified by the accelerator operator, i.e., a custom specified waveform. A possible example is shown in Fig. 6.

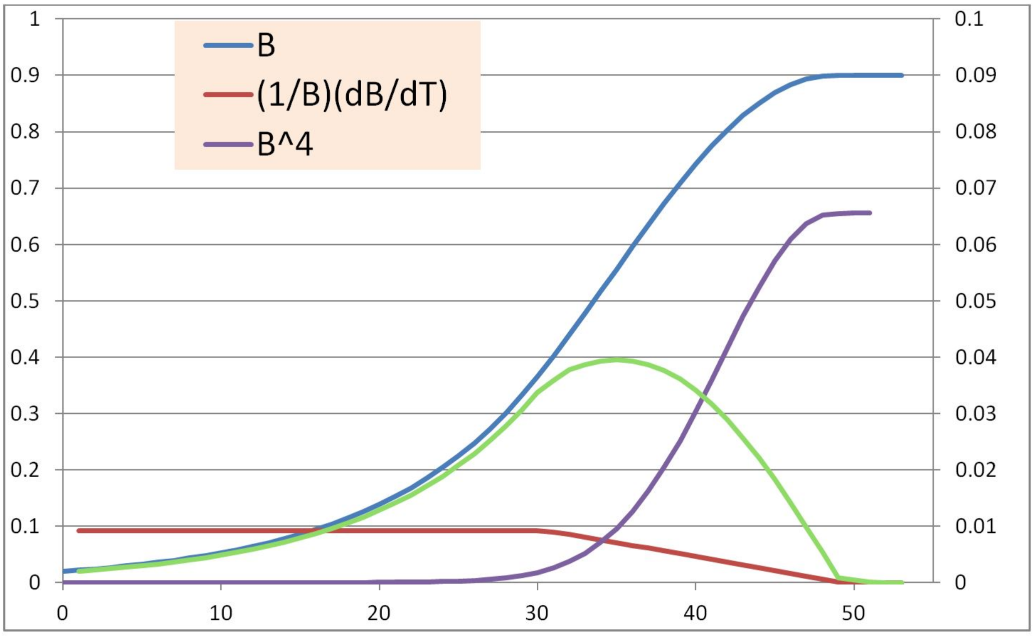

Fig. 6: A 'custom specified' field variation between injection and high energy (extraction) (B), designed to provide a low gradient during and just after injection. Shown is the gradient ($\mathrm{d}B/\mathrm{d}t$), B dot over B [$(1/B)(\mathrm{d}B/\mathrm{d}t)$] and the function determining synchrotron radiation loss (B^4).

The waveform is based on a constant value of $(1/B)(\mathrm{d}B/\mathrm{d}t)$ during and for a significant time after injection, which subsequently declines to zero at peak field. If the accelerated beam were to emit synchrotron radiation, the late increase in the B^4 term would result in a significant reduction in RF power, although the peak RF voltage is increased as the maximum in the $\mathrm{d}B/\mathrm{d}t$ term is higher.

2.2.4 Waveform comparison

A comparison of the three different waveforms presented in Figs. 4, 5, and 6 is given in Table 1.

Table 1: Comparison of suitability of three possible magnet waveforms

Waveform	Suitability
Linear ramp	Gradient constant during acceleration Limited voltage needs in the power supply $(\mathrm{d}B/\mathrm{d}t)/B$ very high at injection and low energy
Biased sine wave	$(\mathrm{d}B/\mathrm{d}t)/B$ maximum soon after injection but much lower than the linear ramp. Very limited control of the waveform during acceleration
Beam optimized waveform	Provides low $(\mathrm{d}B/\mathrm{d}t)/B$ at injection and up to half the wave. Presents engineering challenges such as much more voltage requested in the power supply and across the magnet terminals

It can be seen that the choice of waveform is usually a compromise between different criteria and is often predicated by the electrical engineering circuits that are available; this issue will be discussed later in the paper.

3 Power ratings in cycling systems

3.1 Electrical parameters

Figure 7 shows a typical bending magnet with its equivalent circuit.

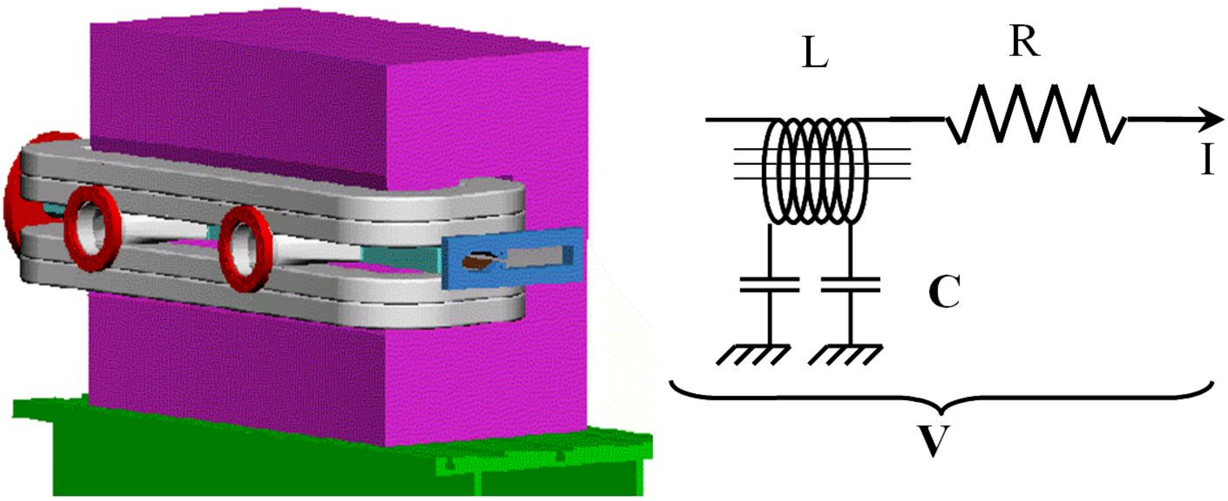

Fig. 7: A typical dipole bending magnet shown with its equivalent circuit

The symbols used in the equivalent circuit are defined below:

- magnet current, I;
- magnet voltage, V;
- series self-inductance, L;
- series resistance, R;
- distributed capacitance to earth, C.

Then:

- magnet voltage,

$$V = RI + L(\mathrm{d}I/\mathrm{d}t); \tag{8}$$

- instantaneous power,

$$VI = RI^2 + LI(\mathrm{d}I/\mathrm{d}t); \tag{9}$$

- stored energy,

$$E = \frac{1}{2}LI^2 \;\rightarrow\; \mathrm{dE/dt} = LI(\mathrm{d}I/\mathrm{d}t); \tag{10}$$

- therefore power,

$$VI = RI^2 + \mathrm{d}E/\mathrm{d}t; \tag{11}$$

The first term in Eq. (11) will be recognized as the resistive loss in the magnet; the second is the rate of change of energy stored in the magnet as the field cycles between injection and peak field. This is referred to as 'reactive power', i.e., it represents a flow of energy which alternates between positive and negative values. The challenge of the cyclic power converter is to control this flow of energy and provide the necessary storage system as significant quantities of energy circulate between the magnet and the power supply.

3.2 Categories of cycling systems

Before examining the various circuits and techniques which are used for power cycling accelerators, it is beneficial to consider the different regimes required for different accelerator applications.

Cycling systems can be categorized according to their repetition rates.

- Slow cycling: the term is usually applied to power systems with cycling time in the range
- 1 s to 10 s; a typical figure would be a cycle time of the order of 3 s. The supply systems for the largest proton accelerators generally fall into this category, as the energy stored in the long chain of electromagnets produces a large reactive power rating even at the low repetition rates.
- Medium cycling: with cycling time from 200 ms to 1 s, such systems have come to prominence more recently due to developments in power electronics which make this frequency range possible with full-waveform controlled circuits (as discussed in the following). They are typically used in separated-function electron accelerators where the lattice configuration eliminates the problem of beam anti-damping at high energy. The main added value is the possibility to use a single- or multi-shot strategy to optimize the stability of the main beam current.
- Fast cycling: corresponding to repetition rates of 10 to 50 Hz, these systems were used in the combined-function electron accelerators in the 1950s and 1960s where rapid acceleration times were needed to limit beam blow-up at high energy. They currently have applications in high-current medium-energy proton accelerators where the rapid cycling time provides intense fluxes of high-energy particles.

Three examples of these different types of accelerator requirements, with corresponding excitation and reactive power ratings, are now presented.

3.2.1 A slow-cycling system: the CERN Super Proton Synchrotron (SPS)

This 450 GeV, slow-cycling accelerator, used for high-energy particle physics, has undergone many modifications during its long life, and currently has a number of different operating modes. The presented data correspond to the ‘fixed-target’ mode, which demands the highest operational parameters. Details of the power system ratings are:

- peak proton energy 450 GeV;
- cycle time (fixed target) 8.94 s;
- peak current 5.75 kA;
- peak $\mathrm{d}I/\mathrm{d}t$ 1.9 kA/s;
- magnet resistance 3.25 Ω;
- magnet inductance 6.6 H;
- magnet stored energy 109 MJ.

The waveforms corresponding to this mode of operation are shown in Figs. 8, 9 and 10.

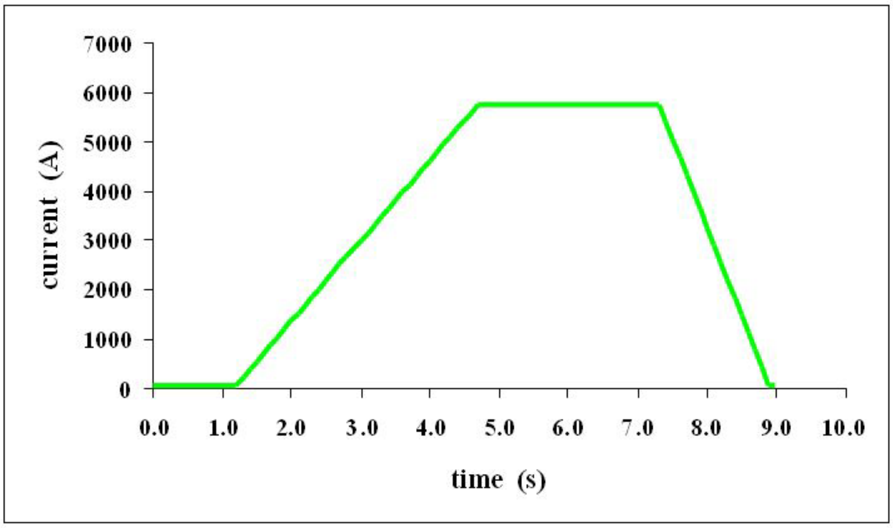

Fig. 8: Current waveform of the CERN SPS when operating in 'fixed-target' mode

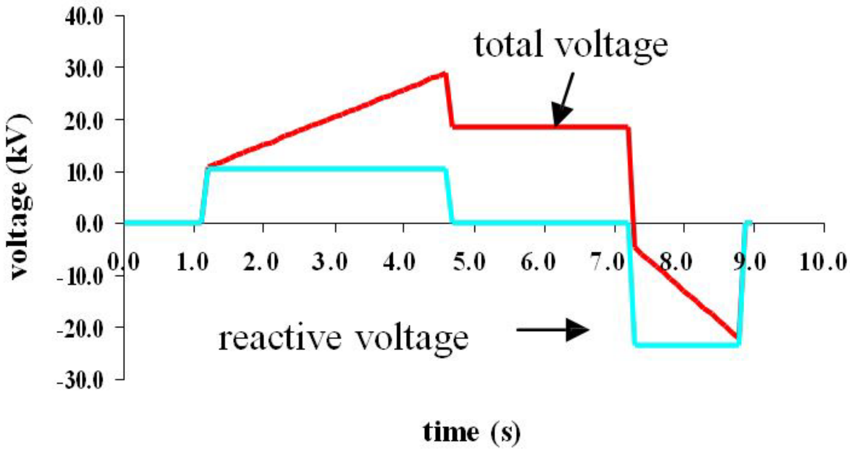

Fig. 9: Voltage waveforms of the CERN SPS corresponding to the current waveform of Fig. 8

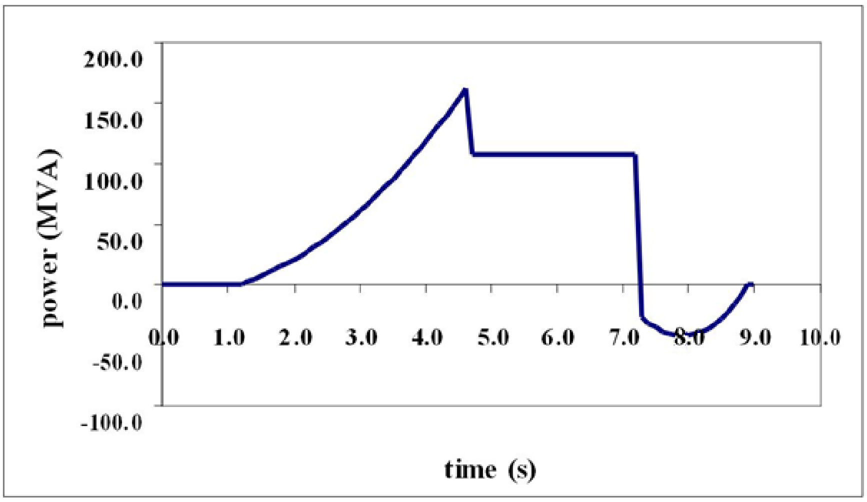

Fig. 10: Power waveform of the CERN SPS corresponding to the excitation levels shown in Figs. 8 and 9

It can be seen that the oscillation of energy between supply and load calls for forward voltages of 30 kV and reverse voltages of 20 kV. However, Fig. 9 demonstrates that the resistive voltage dominates during the acceleration and the flat-peak-field part of the cycle; reactive power is small compared to the resistive loss. Thus, the reverse power shown in Fig. 10 is small compared to the forward power in the earlier part of the cycle; however, the reverse power is still of the order of 50 MVA.

3.2.2 A fast-cycling system: the European Synchrotron Radiation Facility (ESRF) booster

The ESRF is a medium-sized electron storage ring which generates synchrotron radiation for a wide range of research applications; it has a full energy (6 GeV), 10 Hz (fast-cycling) booster synchrotron which accelerates electrons for injection into the main ring. The parameters of the booster's power system are as follows:

– peak electron energy	6.04 GeV;
– cycle time	100 ms;
– cycle frequency	10 Hz;
– peak dipole current	1467 A;
– magnet resistance	568 mΩ;
– magnet inductance	178 mH;
– magnet stored energy	191 kJ.

The power systems waveforms are shown in Figs. 11 and 12.

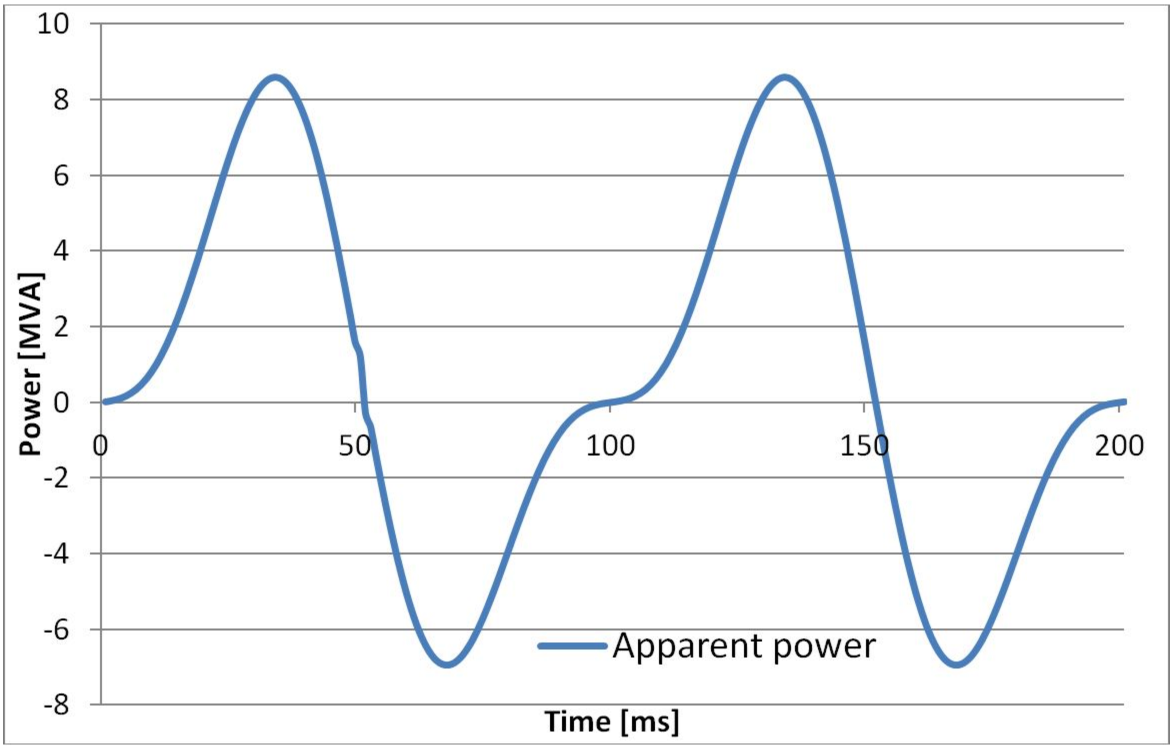

Fig. 11: Current waveform of the ESRF booster, and resistive and total voltage waveforms of the ESRF booster synchrotron.

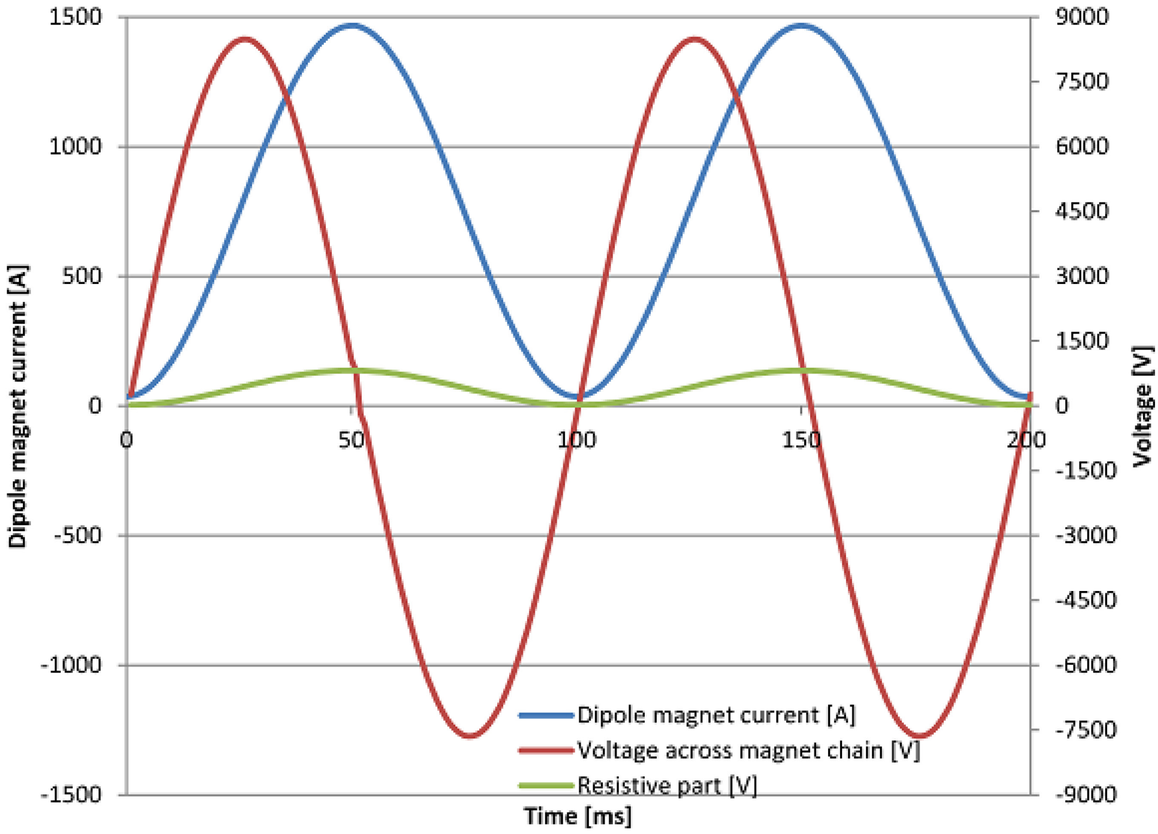

Fig. 12: Power waveform of the ESRF booster corresponding to the excitation levels shown in Fig. 11

It can be seen that the reactive voltage greatly exceeds the resistive voltage; the energy stored is more than an order of magnitude greater than the loss per cycle. Consequently, the power waveform is far more symmetrical about the time axis, compared to the SPS data, and energy storage is a vital feature of this power system's performance.

4 Cycling converter systems

Having examined the ratings of various cycling accelerators, it is now possible to discuss the nature of the power systems used to excite the magnet circuits. As the energy storage system is fundamental to the design, the various circuits can be categorized according to the elements used for this purpose. They fall into three categories:

– mechanical energy storage;
– inductive energy storage;
– capacitive energy storage.

When considering the circuits that need to be assembled around the central storage device, it is worthwhile emphasizing the basic requirements. The power converter system should:

– provide a unidirectional alternating waveform;
– provide accurate control of waveform amplitude;
– provide accurate control of waveform timing;
– provide storage of magnetic energy during low field for efficiency purposes;
– avoid disturbances on the neighbouring customers;

– if possible, provide waveform control to compensate for magnetic non-linearities;
– if needed (and possible), provide discontinuous operation for 'top-up mode'.

4.1 Storing energy locally

One of the difficulties that influences the choice of the converter is to be as transparent to the supply network as possible. The large energy exchange with the public network is the potential cause of disturbances: this low-frequency perturbation is called the 'flicker'.

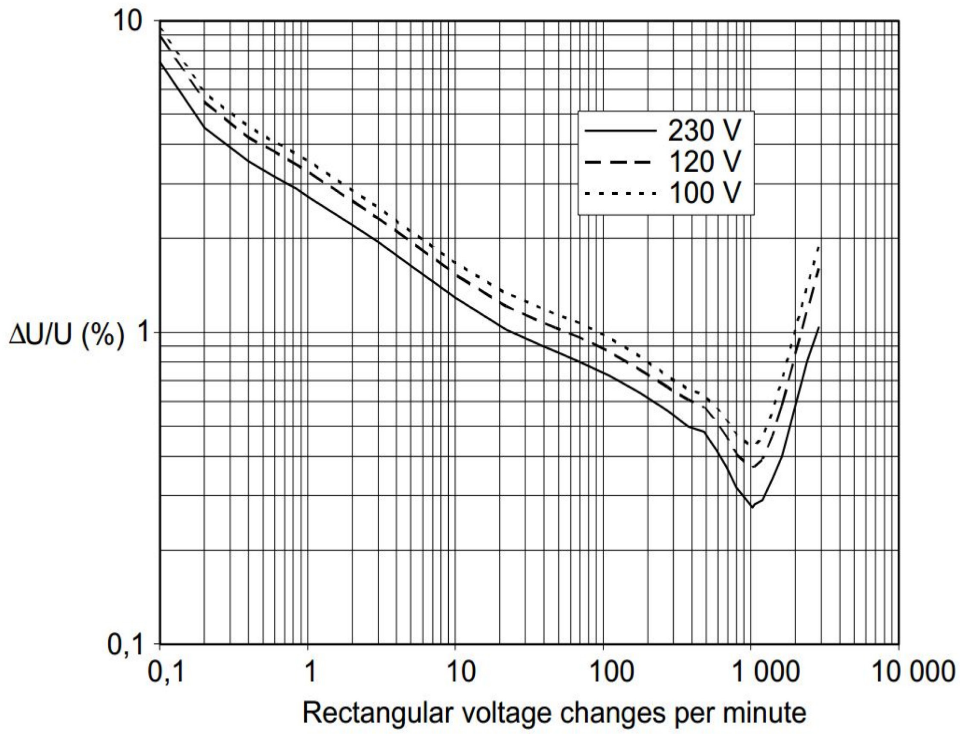

Fig 13: Curve of the maximum variation of supply voltage authorized on European networks. Note that two consecutive voltage changes (one positive and one negative) constitute one 'cycle', i.e., two voltage changes per second mean a 1 Hz fluctuation.

The worst case is at the bottom of the curve: 1200 voltage changes per minute yields 20 changes per second, and this is 10 Hz. The maximum tolerated value at 10 Hz is 0.29%, leading to a request for a public network rigidity 345 times higher than energy exchange. With the example of the ESRF booster dipole magnets, the power fluctuation of 15.5 MVA should produce less than 0.29% $\Delta U/U$ on the local network voltage. The current value at the ESRF on the 20 kV 50 Hz mains short-circuit power is 150 MVA. As a result, this power exchange will therefore produce more than 10% $\Delta U/U$ at 10 Hz. The maximum allowed is 0.29% × 150 MVA = 435 kVA for all systems including quadrupole and RF systems. Storage of magnetic energy during low field for flicker constraint is therefore mandatory to avoid disturbances on the neighbouring customers. The regional transport network at 225 kV–7 GVA short-circuit capacity allows 20 MVA power cycling at 10 Hz, which is just sufficient for the energy exchange requested at the ESRF.

4.2 Slow-cycling mechanical energy storage

These circuits were used to power and control the slow-cycling synchrotrons of the second half of the twentieth century. A diagram of a typical mechanical energy storage system is shown in Fig. 14.

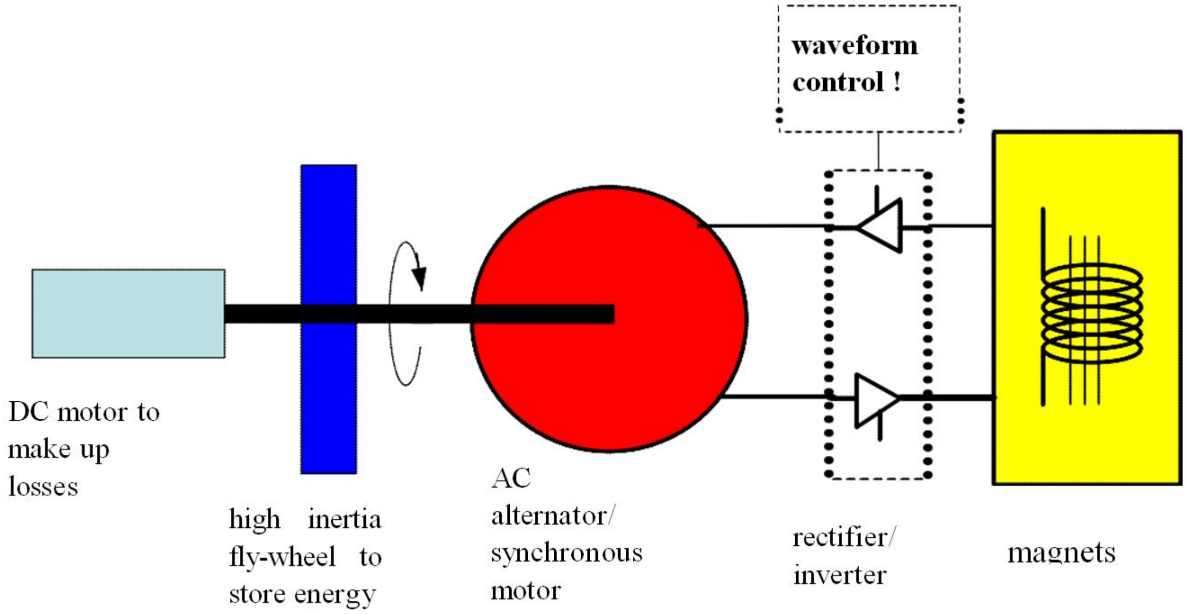

Fig. 14: Diagram of a typical mechanical energy storage system

The use of mechanical energy storage is only suitable for slow-cycling accelerators. Furthermore, the use of rotating machinery resulted in high capital and maintenance costs and, in some cases, the pulse duty caused faults in the alternators. In the later part of the twentieth century, the concept of mechanical storage was replaced by the use of direct connection to large very rigid national and international electrical supply grid systems using the large power plants' alternator inertia.

4.3 Slow-cycling direct connection

National supply networks have large, inductive stored energy. Given the correct interface, this can be utilized to provide and receive back the reactive power of a large accelerator.

Compliance with supply authority regulations must minimize:

– voltage flicker at the feeder with the curve indicated in Fig. 13;

– phase disturbances at the accelerator and neighbouring sites;

– frequency fluctuations over the entire network.

A very 'rigid' (i.e., high short-circuit capacity) high-voltage line into the accelerator equipment is necessary.

4.3.1 The magnet power supply system for the SPS (CERN)

A simplified diagram of this system is given in Fig. 15.

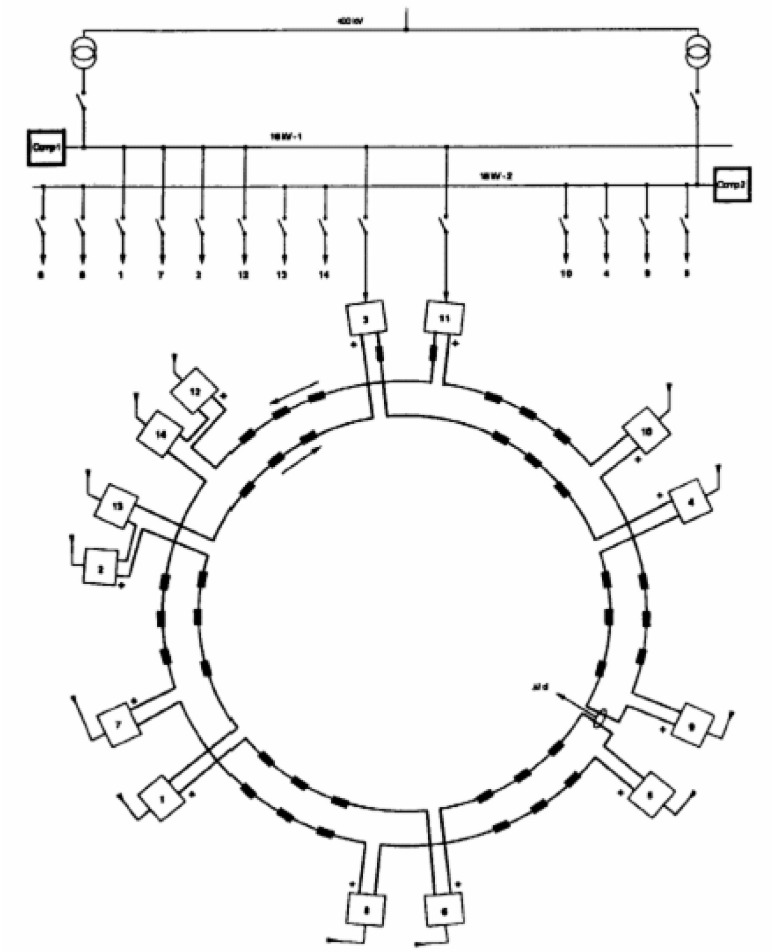

Fig. 15: The directly connected power supply system of the CERN SPS magnets

The diagram shows 14 converter modules, each comprising 2 sets of 12 pulse phase-controlled thyristor rectifiers. These are connected to the ring dipoles in series, with segments of the load located between successive power units; this prevents the required circuit voltage being applied in a single step. Each module is connected to its own 18 kV feeder, which is directly fed from the 400 kV French network.

As with the mechanical energy storage systems, the magnet current is controlled through phase-controlled rectifiers—solid-state thyristors in this case. Hence control of the magnet waveform, within the limitations of the converter's output voltage, is available.

Whilst the direct connection to the extensive and very rigid French grid provides an adequate source and sink of energy, compensation is necessary to prevent excessive phase swings at the CERN site. This is provided by a number of filters using saturable reactors, which are connected to the 18 kV line, as shown in Fig. 16 and also explained in Karsten Kahle's contribution in these proceedings.

This system represents significant capital savings compared to the earlier fly-wheel/alternator system. The maintenance costs and necessary downtime associated with rotating machines are reduced. This is therefore the preferred converter for large, slow-cycling accelerators; the CERN equipment has worked reliably and successfully since the commissioning of the SPS, and other particle physics laboratories have adopted this solution. However, it is strongly dependent on the energy storage characteristics of the local electrical network, on the availability of a very rigid high-voltage supply line, and on the agreement and co-operation of the electrical utility company, linked with rules for anti-flicker constraints.

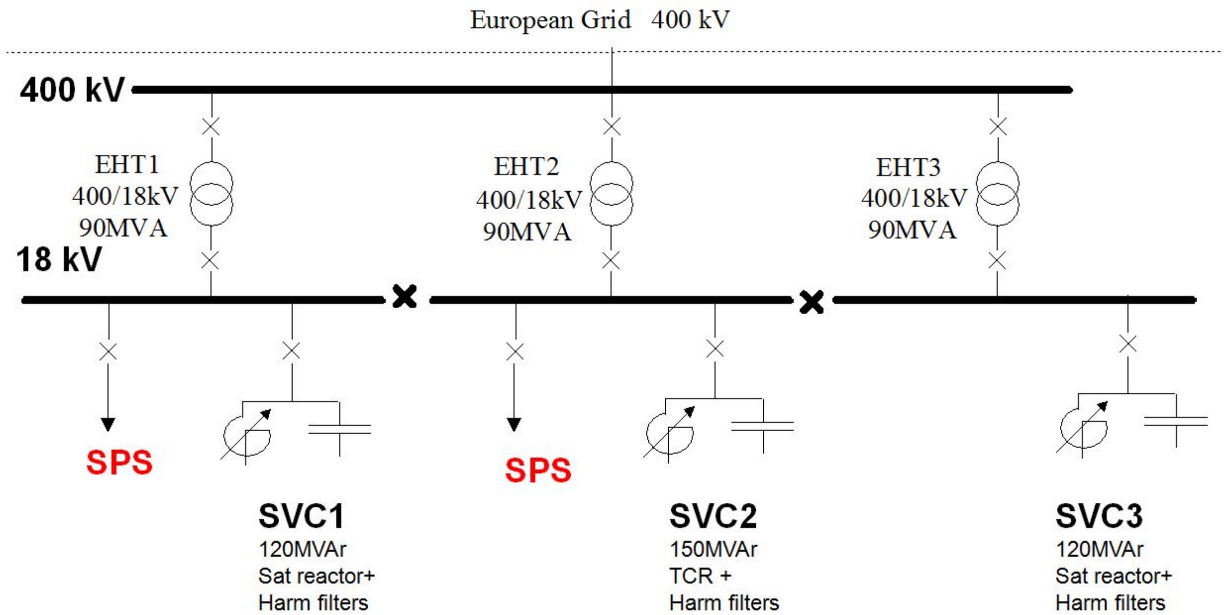

Fig. 16: Connection of filters using saturable reactors to the 18 kV feeder for the SPS magnet power supply system. The filters compensate for the inductive nature of the supply system and minimize phase swings that would otherwise occur, resulting from the power fluctuation during the acceleration and deceleration cycles.

4.4 Medium- and fast-cycling inductive storage systems

Neither mechanical storage nor direct connection is suitable for systems with cycling frequencies much above 1 Hz. Hence the fast- and medium-cycling accelerators (mainly electron synchrotrons) developed in the 1960s and 1970s used inductive energy storage. At that time inductive storage was roughly half the cost per kJ of capacitive energy storage, though this situation changed towards the end of the twentieth century (see the following). The 'standard circuit' was developed originally at the Princeton-Pen accelerator and was named the 'White circuit' after that laboratory's director, Professor Milton White.

4.4.1 The singe-cell White circuit

In its simplest form, the White circuit comprises a complete series string of the accelerator magnets, connected into a parallel network of resonating capacitors and an energy storage inductor. A diagram of such a circuit is given in Fig. 17.

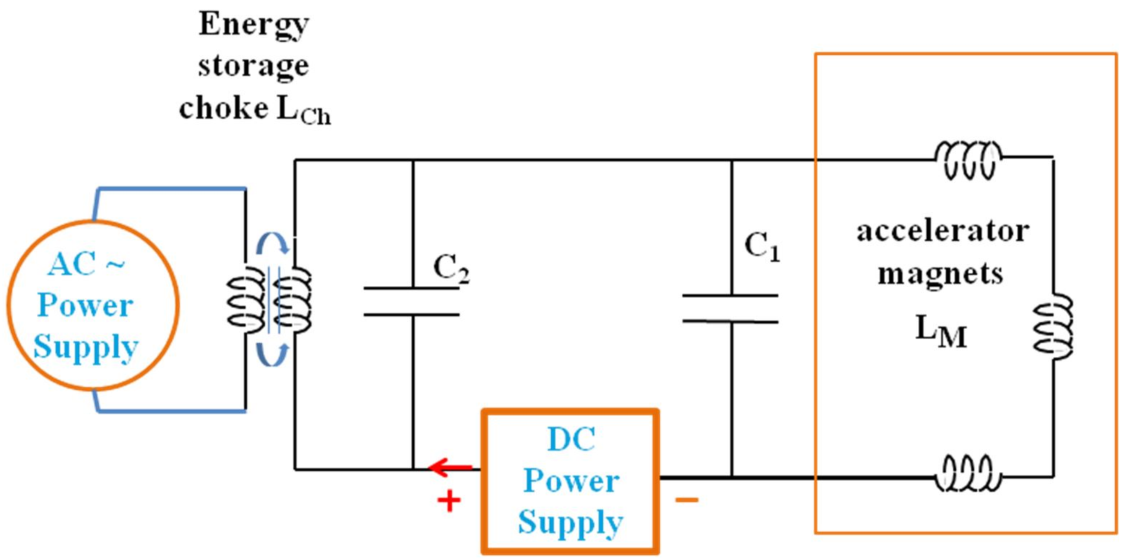

Fig. 17: Schematic diagram of a single-cell 'White circuit'

The series-connected accelerator magnets are resonated at the cycling frequency by capacitance C_1. In parallel with this circuit is another resonant system comprising an inductor, referred to as the 'energy storage choke' and the resonating capacitor C_2. The d.c. converter which generates the direct current required to bias the alternating sine wave is located between these two parallel circuits; providing the two circuits are correctly resonated, there will only be a small alternating current flowing through this rectifier set. The a.c. excitation is provided by an inverter supply powering the parallel circuits by means of a further winding on the inductor, which is closely coupled to the main inductive winding. Again, providing the resonant tunes are correct, the a.c. supply sees a resistive load and, of course, sees no direct current. Consequently, the basic feature of the system is to connect the magnets to two separate supplies—one d.c. and one a.c.—that do not interfere with each other, that are orthogonal in their control functions, and that, together, generate a fully biased sine wave in the accelerator magnets.

These features of the circuit are summarized as follows:

- magnets are all in series—this ensures field uniformity around the accelerator;
- circuit oscillation frequency given by ω;
- C_1 resonates magnet in parallel:
$$C_1 = \omega^2/L_{\mathrm{M}}C_1; \tag{12}$$
- C_2 resonates energy storage choke:
$$C_2 = \omega^2/L_{\mathrm{Ch}}; \tag{13}$$
- the energy storage choke has a primary winding which is closely coupled to the main winding;
- only small a.c. is present in the d.c. source;
- no d.c. is present in the a.c. source;
- the waveform control is very limited to a few per cent of adjustment to compensate saturation effects. This will not be developed here.

A diagram of the current waveform is given in Fig. 18; this defines the parameters used in the following section.

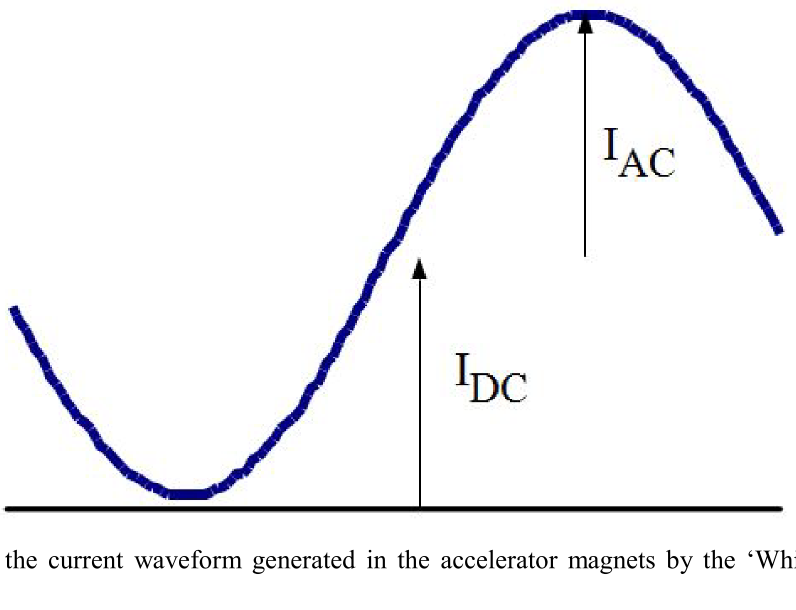

Fig. 18: Diagram of the current waveform generated in the accelerator magnets by the 'White circuit'

The equations corresponding to this circuit are as follows:

– magnet current,
$$I_{\mathrm{M}} = I_{\mathrm{dc}} + I_{\mathrm{ac}} \cdot \sin(\omega t); \tag{14}$$

– magnet voltage,
$$V_{\mathrm{M}} = R_{\mathrm{M}} I_{\mathrm{M}} + \omega I_{\mathrm{M}} L_{\mathrm{M}} \cdot \cos(\omega t); \tag{15}$$

– choke inductance,
$$L_{\mathrm{Ch}} = \alpha L_{\mathrm{M}} \text{ (α is determined by inductor/capacitor economics)}; \tag{16}$$

– choke current,
$$I_{\mathrm{Ch}} = I_{\mathrm{dc}} - (1/\alpha) I_{\mathrm{ac}} \cdot \sin \omega t; \tag{17}$$

– peak magnet energy,
$$E_{\mathrm{M}} = (1/2) L_M \cdot (I_{\mathrm{dc}} + I_{\mathrm{ac}})^2; \tag{18}$$

– peak choke energy,
$$E_{\mathrm{Ch}} = (1/2\alpha) L_{\mathrm{M}} \cdot (I_{\mathrm{dc}} + I_{\mathrm{ac}}/\alpha)^2; \tag{19}$$

– typical values:
$$I_{\mathrm{dc}} \sim I_{\mathrm{ac}};\ \alpha \sim 2. \tag{20}$$

Then,
$$E_{\mathrm{M}} \sim 2 L_{\mathrm{M}} (I_{\mathrm{dc}})^2; \tag{21}$$

$$E_{\mathrm{Ch}} \sim 9/4\, L_{\mathrm{M}} (I_{\mathrm{dc}})^2. \tag{22}$$

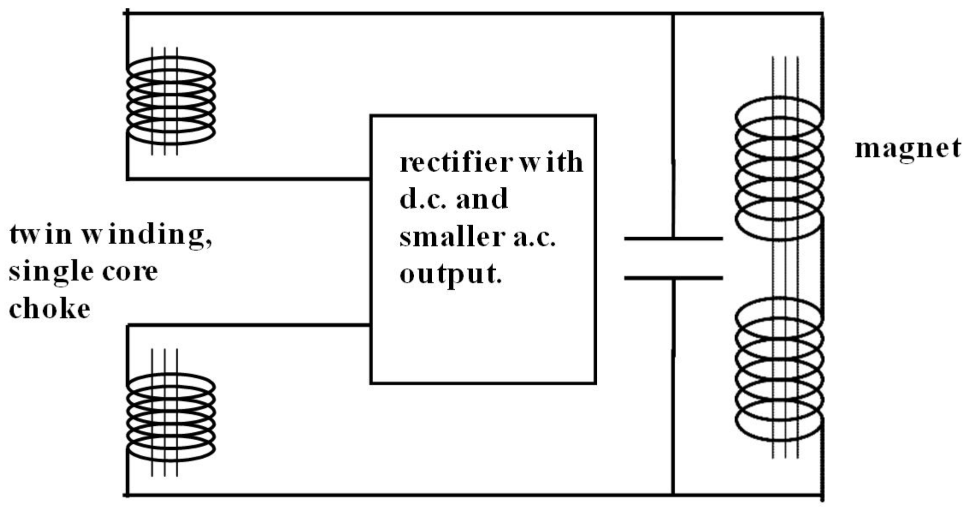

Fig. 19: Modified version of the single-cell White circuit which utilizes a single power source to generate both alternating and direct currents in the magnet.

4.4.2 The multi-cell distributed White circuit

The single-cell White circuit has all magnets series connected and resonated by a capacitor bank, the complete magnet voltage appearing across this single parallel circuit. For large fast-cycling accelerators, where the magnet alternating voltage significantly exceeds 10 kV, it is necessary to divide the White circuit into a number of separate cells, which are series connected, with a capacitor/choke parallel circuit separating each cell. Such an arrangement is shown in Fig. 20.

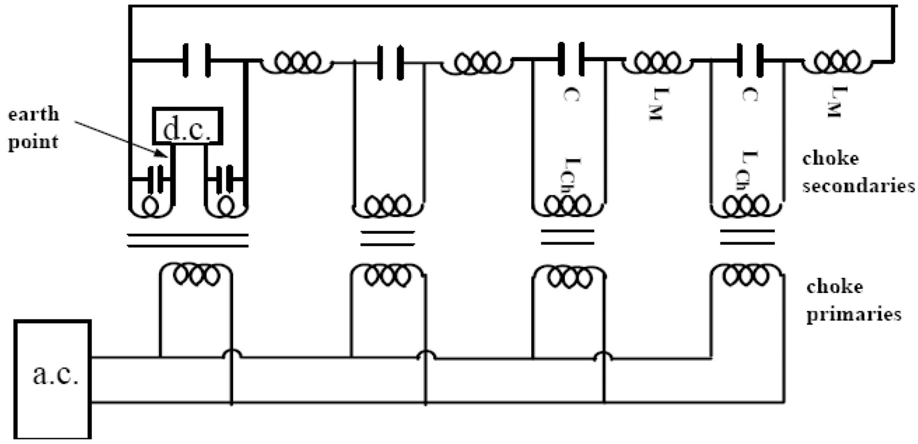

Fig. 20: The distributed White circuit arrangement, as required when the magnet series alternating voltage would be excessively high across a single cell; the example shown is a four-cell circuit.

The nomenclature used in Fig. 20 is as defined in Section 4.3.1, with the magnets identified as L_M. It can be seen that these are still series connected to ensure current continuity. The diagram is for a four-cell system but, in principle, the circuit can be assembled with any number of cells as required to limit the voltages to earth (see the following).

The energy storage choke is now divided into a number of separate secondary windings, each closely coupled to a corresponding primary. One secondary winding is further divided into two, with the source of the d.c. bias located at this point, which is also made the single firm earth point in the network. The capacitance in the circuit is also segmented, with a bank connected in parallel with each secondary; each bank combines the magnet and choke capacitances (C_1 and C_2 of Fig. 17). At the split secondary, the capacitances that resonate the choke in parallel and the magnets in series are separated. With these provisos, the equations of Section 4.3.1 for the single-cell circuit are equally valid for this circuit.

The primary windings are all connected in parallel; this prevents unwanted 'spurious modes of resonance' which can occur when multiple resonant systems are coupled. With primary windings absent, a four-cell secondary network has spurious resonances which are the four eigenvalues ω_n predicted by the following equation:

$$\begin{pmatrix} 1 \\ 1 \\ 1 \\ 1 \end{pmatrix} - \omega_n^2 L_{\text{Ch}} \begin{pmatrix} K_{1,1} & K_{1,2} & K_{1,3} & K_{1,4} \\ K_{2,1} & K_{2,2} & K_{2,3} & K_{2,4} \\ K_{3,1} & K_{3,2} & K_{3,3} & K_{3,4} \\ K_{4,1} & K_{4,2} & K_{4,3} & K_{4,4} \end{pmatrix} \begin{pmatrix} C_1 & 0 & 0 & 0 \\ 0 & C_2 & 0 & 0 \\ 0 & 0 & C_3 & 0 \\ 0 & 0 & 0 & C_4 \end{pmatrix} = 0 \qquad (23)$$

where

- K_{nm} are coupling coefficients between choke windings n, m;
- C_n is capacitance n;
- L_{Ch} is self-inductance of each secondary;
- ω_n are the frequencies of spurious modes.

The spurious modes do not induce magnet currents but can represent a serious energy loss mechanism in the circuit; hence, the use of closely coupled parallel-connected choke primaries is strongly advisable.

The use of paralleled primaries also ensures that the voltages across each section are equalized—an arrangement that prevents the alternating currents *at the fundamental frequency of oscillation* that pass through stray capacitances to earth resulting in dissimilarity of magnet current around the network. Given this equalization of voltage across each section, the voltage distribution to earth along the magnet and choke secondary circuit is as shown in Fig. 21 (for clarity, the primary windings are not shown). It can be seen that the multi-cell arrangement prevents the magnet voltages accumulating to a level that would provide difficulty with coil and bus-bar insulation.

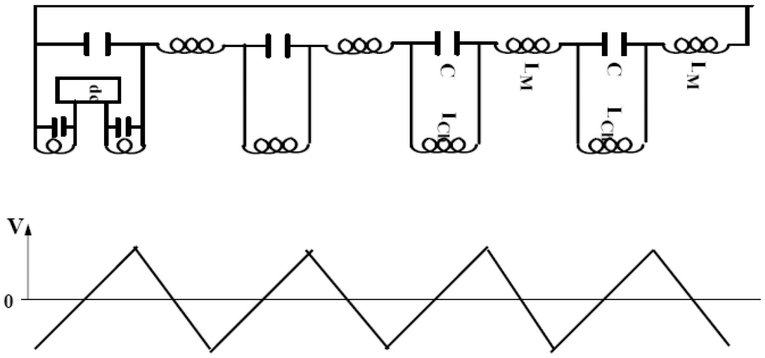

Fig. 21: Voltage distribution to earth in the secondary circuit of the multi-cell White circuit

The principle features of an *n*-cell White circuit are summarized as follows:

- the magnets are still in series for current continuity and equity;
- the voltage across each section is only $1/n$ of the total magnet voltage;
- the maximum voltage to earth is only $1/2n$ of the total;
- the choke has to be split into *n* separate windings;
- the d.c. supply is at the centre of one split secondary winding—this is the circuit's firm earth point;
- the a.c. is connected through a paralleled primary;
- the paralleled primary must be close coupled to the secondary to balance voltages in the circuit;
- there is *no* waveform control.

An example is shown in Fig. 22.

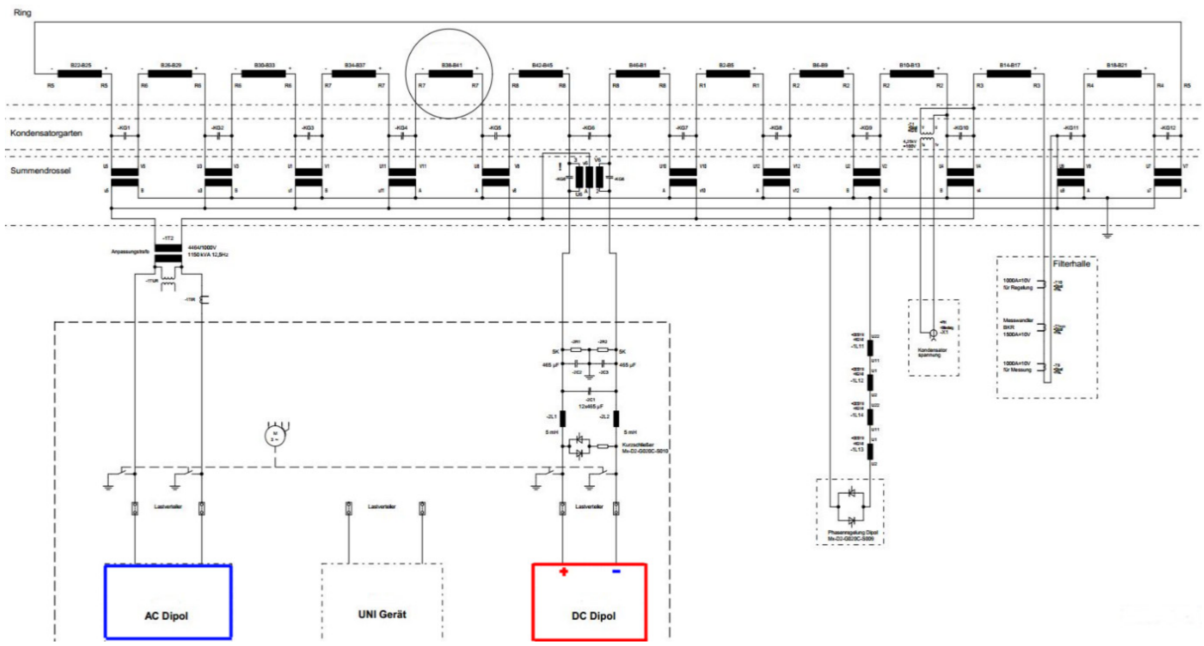

Fig. 22: Desy 12.5 Hz booster synchrotron example

4.5 Modern capacitive energy storage systems with switch-mode control

Technical and economic developments in electrolytic capacitor manufacturing now result in capacitive energy storage being of lower cost than inductive energy storage (providing voltage reversal is not required). Additionally, semiconductor technology now allows the use of fully controlled devices (Insulated Gate Bi-polar Transistors—IGBTs) giving waveform control at medium current and voltages, using the 'switch mode' principle. Medium-sized synchrotrons with cycling times of 1–5 Hz can now take advantage of these developments for cheaper and dynamically controllable power magnet converters, with waveform control available, within the limits of the current and voltage ratings. This innovation was pioneered by Irminger, Horvat, Jenni and Boksberger at the Swiss Light Source (SLS); the *single line equivalent* circuit that they developed to power the 3 Hz booster synchrotron is shown in Fig. 23.

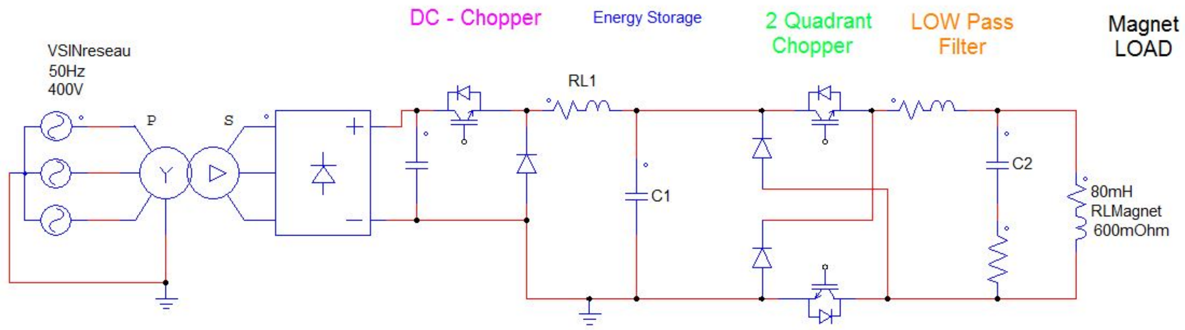

Fig. 23: Controlled capacitive energy storage system developed for the SLS

The accelerator magnets (identified as LOAD in Fig. 23) are series connected and are fed in reality by two power converter circuits, each comprising:

- a d.c. power source;
- a d.c. chopper, which controls the flow of energy to make up the system losses;
- the main energy storage capacitor;
- a high-frequency 'switch-mode' chopper circuit which is capable of transferring energy into the magnet, allowing the load to 'free-wheel' in a passive state or inverting the energy flow and recharging the capacitor from the energy stored in the magnet;
- a number of low-pass filters, which smooth out the chopping ripple and deliver the low-frequency voltage waveform to the magnet.

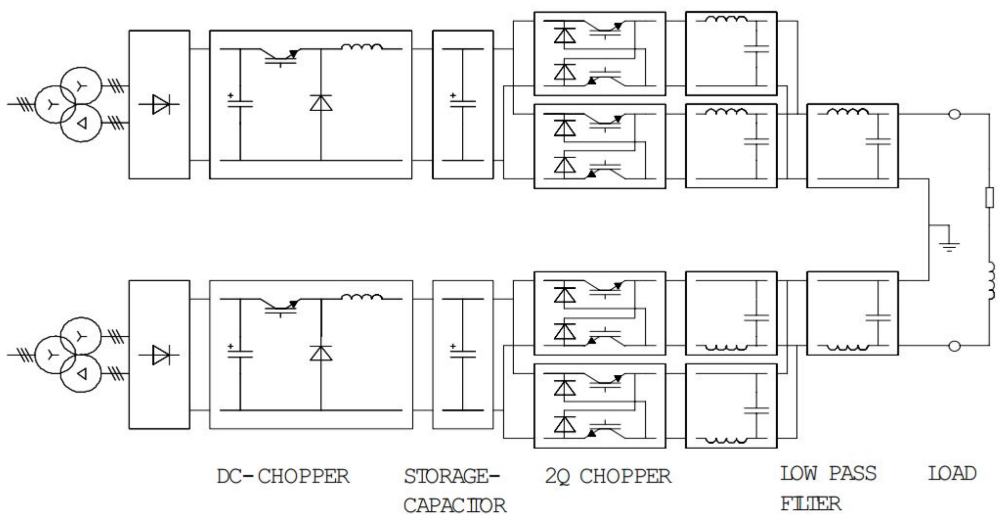

Fig 24: Real power circuit diagram

Each power unit carries half the current, i.e. 475 A and half the voltage, i.e., 500 V. The basic parameters of the SLS booster installation are given in Table 2.

Table 2: Parameters of the SLS booster synchrotron power supply system

Combined-function dipoles	48 BD; 45 BF
Resistance	600 mΩ
Inductance	80 mH
Maximum current	950 A
Stored energy	28 kJ
Cycling frequency	3.1 Hz

The waveforms associated with this circuit are shown in Fig. 25 (magnet current and voltage), Fig. 26 (total power into the magnet) and Fig. 27 (capacitor voltage and input current).

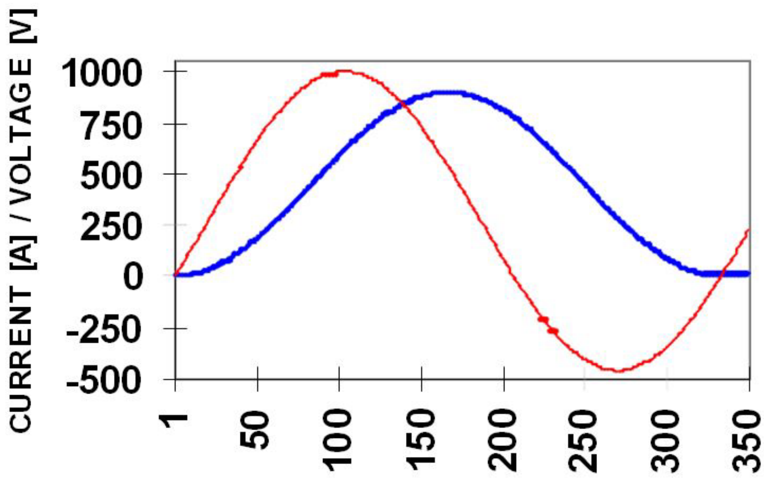

Fig. 25: Magnet current and voltage vs time (ms) in the SLS booster capacitive energy storage power supply system.

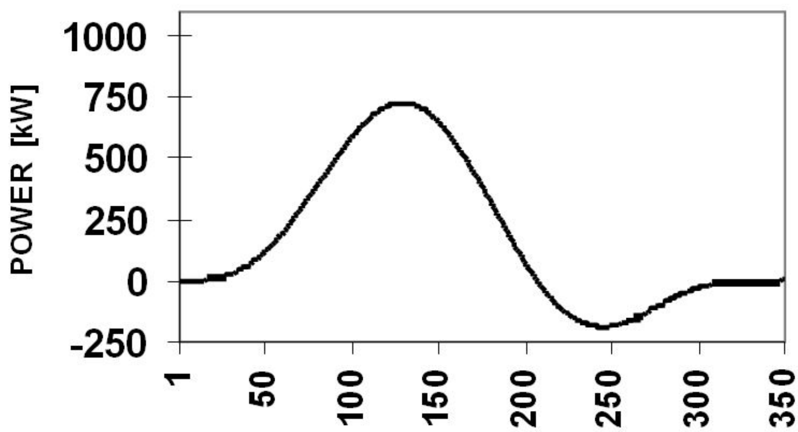

Fig. 26: Magnet power vs time (ms) in the SLS booster capacitive energy storage power supply system

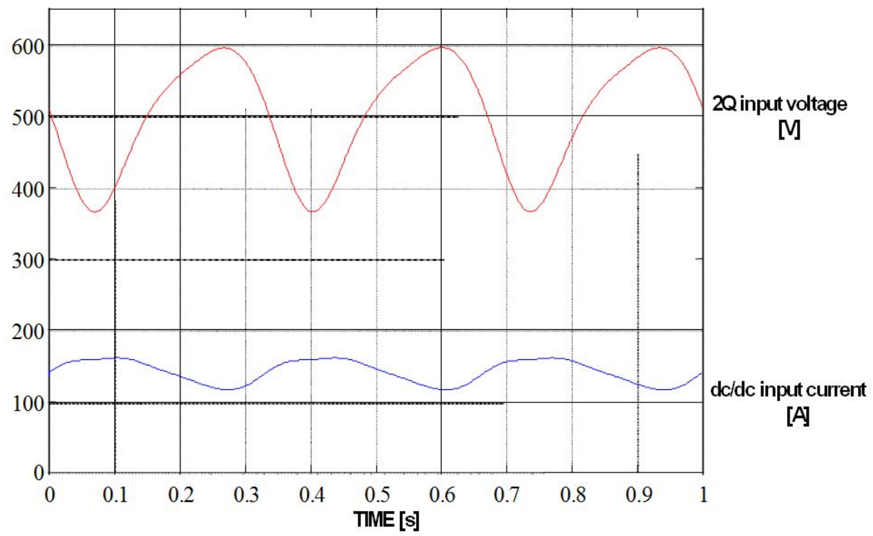

Fig. 27: Capacitor voltage and input current vs time in the SLS booster capacitive energy storage power supply system.

It should be noted that it is the development of the power IGBT that allows this switch-mode circuit to control the magnet waveform. The switching of the high-frequency chopper controls both the direction and the rate of flow of energy between the capacitor and the magnet, and this is only possible in the frequency domain of a few hertz with the use of the power semiconductors, which can switch on and off whilst conducting currents of the order of hundreds of amperes.

It is instructive to contrast this relatively new solution to powering a cycling synchrotron with the older White circuit:

– the switch-mode circuit does not need a costly energy storage choke with increased power losses;

– within limits of rated current and voltage, the switch-mode circuit provides flexibility of output waveform;

– after switch-on, the switch-mode circuit requires less than 1 s to stabilize (valuable in 'top-up mode').

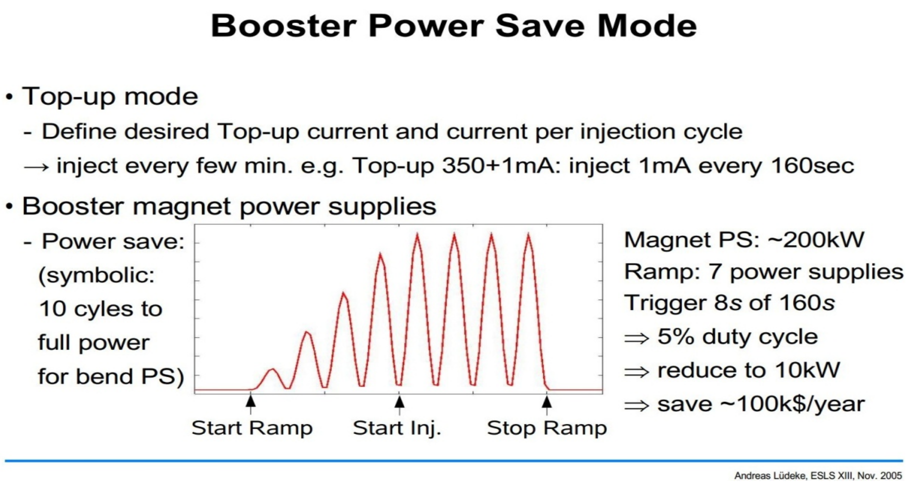

Fig. 28: An example from the SLS of the booster power save mode

The example shown in Fig. 28 from the SLS indicates an increase in efficiency of the injector of such an equipped machine. However, the current and voltages possible in switched circuits are currently restricted by component ratings. The power stress of the silicon die at a few hertz is the major difficulty to overcome for such power converters.

The booster synchrotrons of the next generation of light sources (Soleil, Diamond) are using this circuit, with component ratings now adequate to power the 3 GeV, 5 Hz booster for Diamond. However, the use of such a circuit for a 50 Hz fast-cycling accelerator is still some way off, and capacitor and IGBT voltage ratings will need to rise by approximately an order of magnitude before this becomes realistic.

5 Case of slow-cycling Pulse Width Modulation (PWM) with integrated capacitive storage

The CERN power converter for the Proton Synchrotron (PS) accelerator was powered by a rotating machine sized to 90 MVA. This system, described by Fig. 29, enables an acceptable energy exchange between magnets and mechanical storage to avoid exchange with the public network.

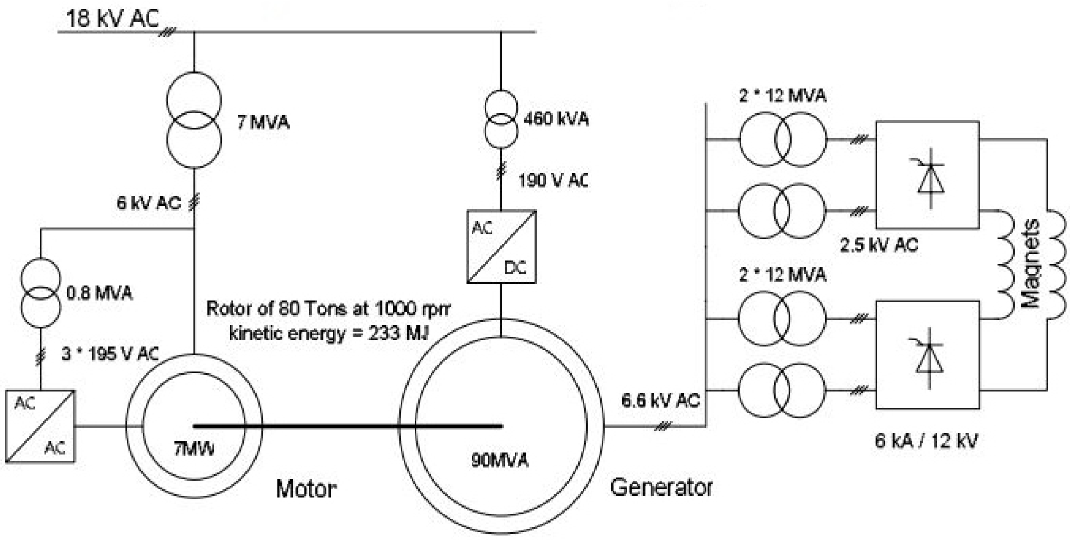

Fig. 29: Single line diagram of the 90 MVA electro kinetic system powering the PS at CERN

The basic data for the magnet are as follows: ±10 kV, 6 kA, 2.4 s pulse see Fig. 30

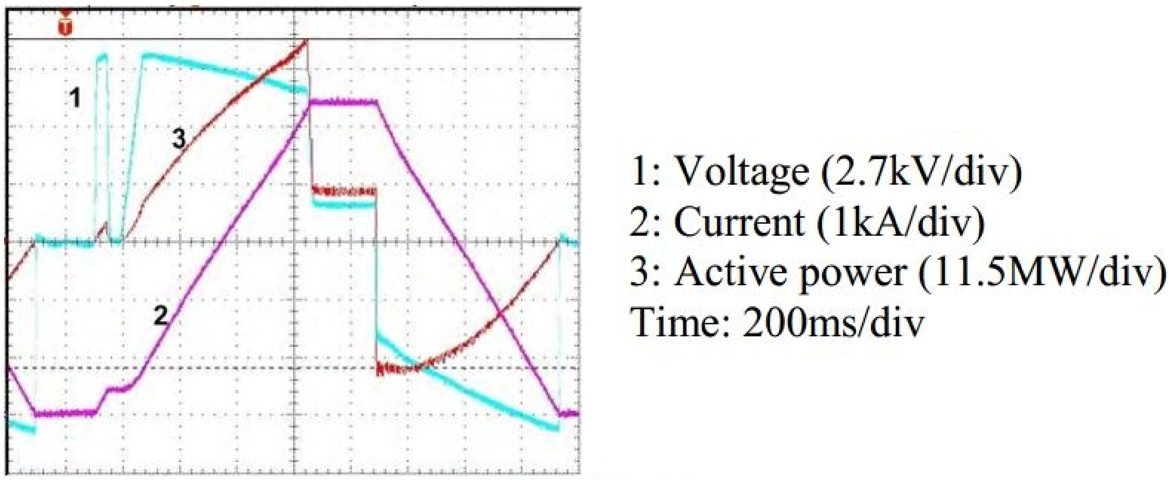

Fig. 30: Typical electrical waveform of the CERN PS accelerator magnets

In 2007 the mechanical storage was replaced by capacitive storage. Figure 31 is a global view of the single line diagram of such a system.

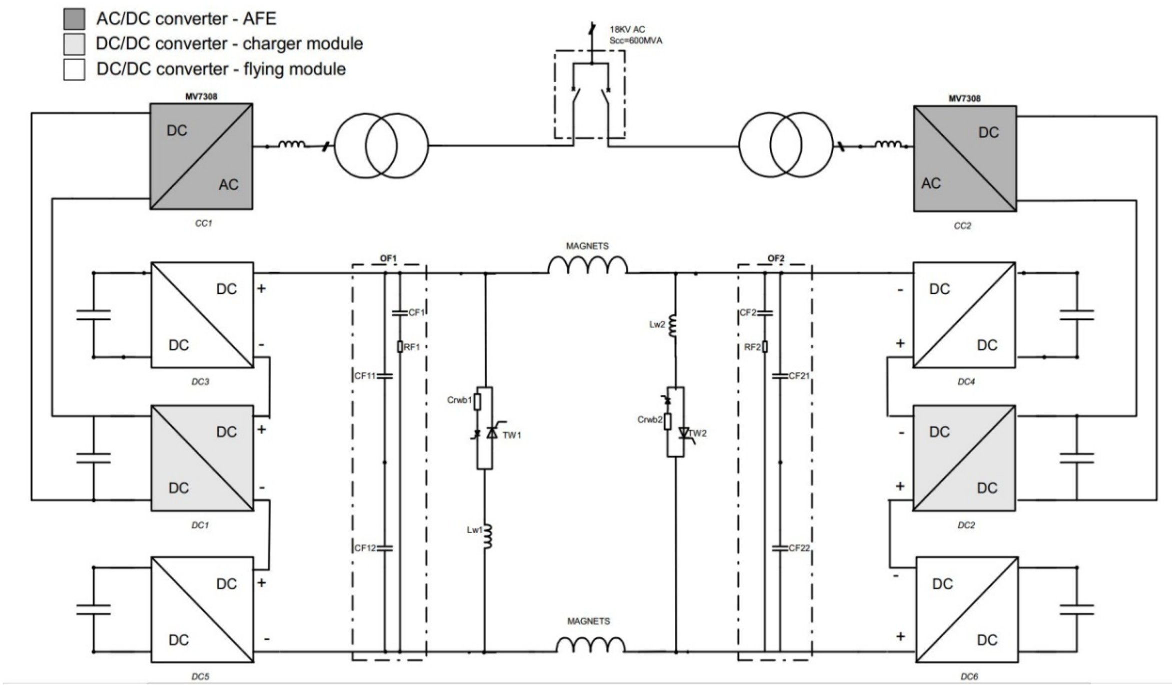

Fig 31: General view of the single line diagram of POPS

Each leg is based on three parallel neutral clamped legs allowing the production of three voltage levels to the output: (+VDC/2, 0, −VDC/2). The six capacitor banks are located in containers (40 ft shelters). Each of them contains 126 units parallel connected for a total value of 0.25 F, 5 kV. The 3 MJ of energy stored can vary from 5 kV to 2 kV, giving 2.5 MJ usable energy exchange. Six capacitor banks in total give 15 MJ of energy available to exchange with the magnet chain. The diagrams of Fig. 32 show the main current and voltage of such a system.

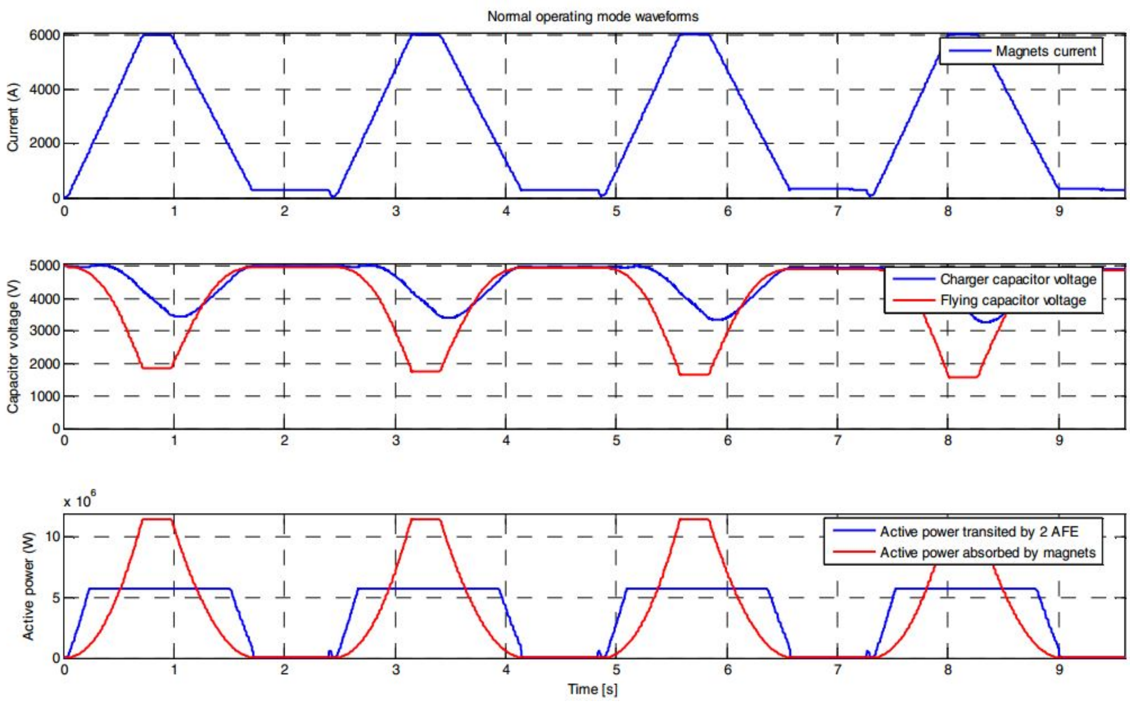

Fig. 32: Main current and voltage diagram of the magnet and capacitor storage elements

6 Conclusion

The power converters are a vital part of a cycling accelerator, and the operational efficiency and susceptibility of the machine to parameter drift are dependent on the stability and accuracy of the converters and whether their waveform can be adjusted to match the beam requirements during acceleration. It is therefore important that the engineers designing and operating the converters are in close collaboration and communication with the magnet designers and those defining the lattice and predicting the beam behaviour. In this way the most suitable circuit will be chosen and the optimum performance obtained.